

Solution for jump conditions at fast shocks in an anisotropic magnetized plasma

N. V. ERKAEV,¹ D. F. VOGL^{2,3} and H. K. BIERNAT^{2,3,4}

¹Institute of Computational Modelling, Russian Academy of Sciences,
Krasnoyarsk 660036, Russia

²Space Research Institute, Austrian Academy of Sciences,
Schmiedlstraße 6, A-8042 Graz, Austria

³Also at: Institute for Geophysics, Astrophysics, and Meteorology, University of Graz,
Universitätsplatz 5, 8010 Graz, Austria

⁴Also at: Institute for Theoretical Physics, University of Graz,
Universitätsplatz 5, 8010 Graz, Austria

(Received 1 December 1999 and in revised form 17 June 2000)

Abstract. We study the magnetic field and plasma parameters downstream of a fast shock as functions of normalized upstream parameters and the rate of pressure anisotropy (defined as the ratio of perpendicular to parallel pressure). We analyse two cases: with the shock (i) perpendicular and (ii) inclined with respect to the magnetic field. The relations on the fast shock in a magnetized anisotropic plasma are solved taking into account the criteria for the mirror instability and firehose instability bounding the pressure anisotropy downstream of the shock. Our analysis shows that the parallel pressure and the parallel temperature as well as the tangential component of the velocity are the parameters that are most sensitive to the rate of pressure anisotropy. The variations of the other parameters, namely density, normal velocity, tangential component of the magnetic field, perpendicular pressure, and perpendicular temperature are much less pronounced, in particular when the perpendicular pressure exceeds the parallel pressure. The variations of all parameters increase substantially for a very low rate of anisotropy, which is bounded by the firehose instability in the case of inclined shocks. Using the criterion for mirror instability as a closure relation for the jump conditions at the fast shock, we obtain the plasma parameters and the magnetic field downstream of the shock as functions of the Alfvén Mach number. For each Alfvén Mach number, the criterion for mirror instability determines the minimum jumps in such parameters as density, tangential magnetic field component, parallel pressure, and temperature, and determines the maximum values of the velocity components and the perpendicular temperature. Ideal anisotropic magnetohydrodynamics (MHD) has wide applications for space plasma physics. Observations of the field and plasma behaviour in the solar wind as well as in the Earth's magnetosheath have highlighted the need for an MHD model where the plasma pressure is treated as a tensor.

1. Introduction

More than four decades ago, Chew, Goldberger, and Low (1956), derived the quasi-magnetohydrodynamic (MHD) equations with a non-isotropic pressure tensor in

application to a collisionless magnetized plasma. This pressure tensor is determined by the magnetic field strength, i.e.

$$P_{ik} = p_{\perp} \delta_{ik} + (p_{\parallel} - p_{\perp}) \frac{B_i B_k}{B^2}. \quad (1.1)$$

The theory of Chew, Goldberger and Low is applicable when the Larmor radius is much smaller than the spatial scale of variations of the plasma parameters. The anisotropic plasma pressure tensor is characterized by two scalar parameters, p_{\parallel} and p_{\perp} , which are the plasma pressures parallel and perpendicular to the magnetic field. This approach is known as a double adiabatic theory because both pressure components are related to the plasma density and the magnetic field strength by two adiabatic equations,

$$\frac{d}{dt} \left(\frac{p_{\parallel} B^2}{\rho^3} \right) = 0, \quad \frac{d}{dt} \left(\frac{p_{\perp}}{\rho B} \right) = 0. \quad (1.2)$$

This theory has been used by a number of authors (Abraham-Shrauner 1967; Lynn 1967; Neubauer 1970) to describe discontinuities in a collisionless plasma. For example, Abraham-Shrauner (1967) derived the general jump conditions for discontinuities in a collisionless plasma in the Chew–Goldberger–Low approximation. Lynn (1967) made a qualitative analysis of the jump conditions for the change in plasma parameters between two stationary, uniform plasma regions, and specified them as contact, tangential, rotational discontinuities, and compressible shocks. For the latter, the coplanarity theorem was proved. Neubauer (1970) obtained solutions of the jump relations for shocks moving into a collisionless anisotropic magnetized plasma under the assumption of isotropic conditions downstream of the shock front. Furthermore, Hudson (1970) discussed the types of discontinuities in a magnetohydrodynamic fluid with anisotropic plasma pressure, and gave rules for their identification in the solar wind. The coplanarity theorem is used to distinguish a fast shock from a rotational discontinuity. However, with regard to fast compressible shocks, the system of jump conditions was not solved in the general case of arbitrary anisotropy of the plasma temperature upstream and downstream of the shock.

Thus, the first aim of our paper is to solve the set of general jump equations at a fast shock in an anisotropic magnetized plasma for given parameters upstream of the shock and a given anisotropy rate downstream of the shock. The main problem that arises here is that the jump relations on the shocks are not sufficient to determine the downstream parameters for given upstream parameters. The ratio of the perpendicular and parallel plasma pressures downstream of the shock is an unknown parameter that has to be determined. In principle, this parameter depends on the structure of the shock; however, this is beyond the scope of an MHD model. One reasonable way to estimate the anisotropy of parameter downstream of the shock is to use the criteria for MHD instabilities in an anisotropic plasma (Thompson 1964). The first is the ‘firehose’ instability, which occurs when $p_{\parallel} - p_{\perp} > B^2/4\pi$. The second is the ‘mirror’ instability, which occurs for sufficiently large p_{\perp} , such that $p_{\perp}/p_{\parallel} > 6(1 + B^2/8\pi p_{\perp})$. Here the factor of 6 on the right-hand side of this relation appears only in an MHD treatment of the mirror instability. This factor is absent in the more correct criterion for mirror instability derived in the kinetic description (Tajiri 1967):

$$p_{\perp}/p_{\parallel} > 1 + B^2/8\pi p_{\perp}. \quad (1.3)$$

The second aim of our paper is to use both criteria – for firehose and for mirror instability – additional relations combined with the jump conditions, to determine the limits of the anisotropy rate downstream of the shock. The latter is used to obtain a possible range of magnetic field, plasma density, perpendicular and parallel pressures, velocity, and magnetic field downstream of the shock for different sonic and Alfvén Mach numbers typical of solar-wind conditions.

2. Basic equations

The general jump conditions for an anisotropic plasma are given by Hudson (1970)

$$[[\rho v_n]] = 0, \tag{2.1}$$

$$[[v_n \mathbf{B}_t - \mathbf{v}_t B_n]] = 0, \tag{2.2}$$

$$\left[\left[p_\perp + (p_\parallel - p_\perp) \frac{B_n^2}{B^2} + \frac{B_t^2}{8\pi} + \rho v_n^2 \right] \right] = 0, \tag{2.3}$$

$$\left[\left[\frac{B_n \mathbf{B}_t}{4\pi} \left(\frac{4\pi(p_\parallel - p_\perp)}{B^2} - 1 \right) + \rho v_n \mathbf{v}_t \right] \right] = 0, \tag{2.4}$$

$$\left[\left[\rho v_n \left(\frac{\mathcal{E}}{\rho} + \frac{v^2}{2} + \frac{p_\perp}{\rho} + \frac{B_t^2}{4\pi\rho} \right) + \frac{B_n^2 v_n}{B^2} (p_\parallel - p_\perp) - \frac{(\mathbf{B}_t \cdot \mathbf{v}_t) B_n}{4\pi} \left(1 - \frac{4\pi(p_\parallel - p_\perp)}{B^2} \right) \right] \right] = 0, \tag{2.5}$$

$$[[B_n]] = 0, \tag{2.6}$$

where ρ is the mass density, \mathbf{v} is the velocity, and \mathbf{B} is the magnetic field strength, with subscripts t and n indicating tangential and normal components with respect to the discontinuity. p_\perp and p_\parallel are the elements of the plasma pressure tensor perpendicular and parallel to the magnetic field. \mathcal{E} is the internal energy, $\mathcal{E} = p_\perp + \frac{1}{2}p_\parallel$. The notation $[[Q]] = Q_2 - Q_1$, is used, with subscripts 1 and 2 indicating quantity Q upstream and downstream of the discontinuity. Equations (2.1)–(2.6) refer to the conservation of physical quantities, i.e. the mass flux, the tangential component of the electric field, the normal and tangential components of the momentum flux, the energy flux, and, finally, the normal component of the magnetic field.

In our calculations, we deal with two dimensionless parameters, A_s and A_m , which are determined for upstream conditions as $A_s = p_{\perp 1} / \rho_1 v_1^2$ and $A_m = 1 / M_a^2$, where M_a is the Alfvén Mach number. The strength of the magnetic field is given by $B_1 = \sqrt{4\pi\rho_1 v_1^2 A_m}$, where v_1 is the bulk velocity. We recall that subscript 1 indicates the physical parameters upstream of the discontinuity. For shocks, the tangential components of the electric and magnetic fields are coplanar. Thus the components of the magnetic field are determined as follows:

$$B_{n1} = B_1 \cos \gamma, \quad B_{t1} = B_1 \sin \gamma, \tag{2.7}$$

where γ is the angle between the magnetic field vector and the vector normal to the discontinuity (see Figure 1). The components of the bulk velocity are chosen as

$$v_{n1} = v_1 \cos \alpha \quad \text{and} \quad v_{t1} = v_1 \sin \alpha. \tag{2.8}$$

Here α is the angle between the bulk velocity and the normal component of the

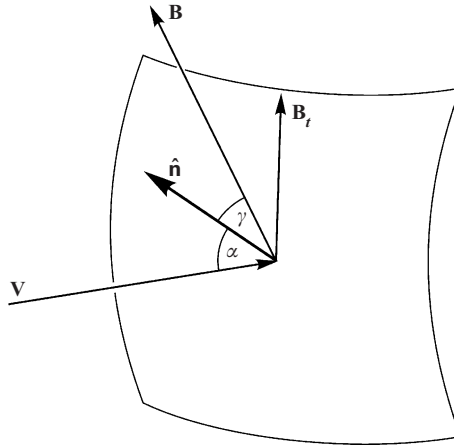


Figure 1. Geometry of the problem.

velocity. In our analysis, we introduce a parameter $\lambda = p_{\perp}/p_{\parallel}$, which determines the pressure anisotropy. Using this parameter, we express the parallel pressure as $p_{\parallel} = p_{\perp}/\lambda$. In particular, the pressures upstream of the discontinuity are given by

$$p_{\parallel 1} = \frac{p_{\perp 1}}{\lambda_1}, \quad p_{\perp 1} = \rho_1 v_1^2 A_s. \quad (2.9)$$

The parameter λ_1 refers to the pressure anisotropy upstream of the discontinuity, and therefore is assumed to be a known quantity.

From the conservation of mass (2.1) and the normal component of the magnetic field (2.6), it consequently follows that

$$\frac{\rho_2}{\rho_1} = \frac{v_{n1}}{v_{n2}} \equiv x, \quad B_{n2} = B_{n1}. \quad (2.10)$$

3. Input parameters

In this section, we define the upstream parameters of the set of equations (2.2)–(2.5). In the following analysis, we consider a coordinate system comoving with the plasma upstream of the shock in the direction parallel to the surface of the discontinuity. Without loss of generality, this simplification leads to $\alpha = 0^\circ$. Taking into account the normalization, $\rho_1 = 1$, $v_1 = 1$, and using the definitions mentioned above, we have the following expressions for the physical quantities upstream of the shock. The tangential component of the electric field, H_1 , is given by

$$H_1 = \sqrt{4\pi A_m} \sin \gamma. \quad (3.1)$$

The normal component of the momentum flux, I_1 , is given by

$$I_1 = A_s + A_s \cos^2 \gamma \left(\frac{1}{\lambda_1} - 1 \right) + \frac{1}{2} A_m \sin^2 \gamma + 1. \quad (3.2)$$

The tangential component of momentum flux, J_1 , is given by

$$J_1 = \frac{1}{2} \sin(2\gamma) \left(\frac{A_s}{\lambda_1} - A_s - A_m \right). \quad (3.3)$$

Finally, the energy flux, W_1 , is given by

$$W_1 = A_s \left(2 + \frac{1}{2\lambda_1} + \frac{\cos^2 \gamma}{\lambda_1} - \cos^2 \gamma \right) + A_m \sin^2 \gamma + \frac{1}{2}. \tag{3.4}$$

4. Solution for the perpendicular shock

First, we study the simpler particular case of the so-called perpendicular shock, where $B_n = 0$. Thus (2.1)–(2.5) reduce to

$$[[\rho v_n]] = 0, \tag{4.1}$$

$$[[v_n \mathbf{B}_t]] = 0, \tag{4.2}$$

$$\left[\left[p_\perp + \frac{B_t^2}{8\pi} + \rho v_n^2 \right] \right] = 0, \tag{4.3}$$

$$[[\rho v_n \mathbf{v}_t]] = 0, \tag{4.4}$$

$$\left[\left[\rho v_n \left(\frac{\mathcal{E}}{\rho} + \frac{v_n^2}{2} + \frac{v_t^2}{2} + \frac{p_\perp}{\rho} + \frac{B_t^2}{4\pi\rho} \right) \right] \right] = 0. \tag{4.5}$$

The quantities downstream of the discontinuity are

$$B_{t2} = x B_{t1}, \tag{4.6}$$

$$v_{t2} = v_{t1}, \tag{4.7}$$

$$p_{\perp 2} = p_{\perp 1} + \frac{B_{t1}^2}{8\pi} (1 - x^2) + \rho_1 v_{n1}^2 \left(1 - \frac{1}{x} \right). \tag{4.8}$$

Substituting (4.6)–(4.8) into the energy equation (4.5) leads to

$$2\lambda_1(3\lambda_2 + 1)y^3 - \lambda_1(4\lambda_2 + 1)(2A_s + A_m + 2)y^2 + \lambda_2[2\lambda_1(4A_s + 1 + 2A_m) + 2A_s]y + A_m\lambda_1 = 0, \tag{4.9}$$

where $y = 1/x$.

Figure 2 shows variations of (a) plasma density, (b) velocity, (c,d) pressures, and (e,f) temperatures downstream of the shock as functions of the anisotropy parameter λ_2 for different Alfvén Mach numbers ranging from 2 to 10. All parameters are normalized to upstream quantities indicated by subscripts 1 as shown in the figure. Parameter A_s , defined as the normalized perpendicular pressure in the inflow region, is equal to 0.01 for all curves on this figure. The thick line appearing in each panel represents the mirror criterion that divides all panels into stable (left side) and unstable (right side) regions. The maximum of the anisotropy parameter, bounded by the mirror instability, increases substantially as M_a decreases.

Density, velocity, parallel pressure, and perpendicular and parallel temperatures are monotonic functions of the anisotropy parameter λ_2 . The exception is the perpendicular pressure, which has a maximum for the curves for large values of M_a ($M_a = 8$ and 10) and a low parameter λ_2 ($\lambda_2 \approx 0.4$).

Figure 3 shows the behaviour of the plasma parameters similar to that of Fig. 2 but for another value of the parameter A_s , namely $A_s = p_{\perp 1} / \rho_1 v_1^2 = 0.04$. The decrease in the parameter A_s brings about changes in the normalized plasma parameters downstream of the shock as follows. The density decreases, the velocity

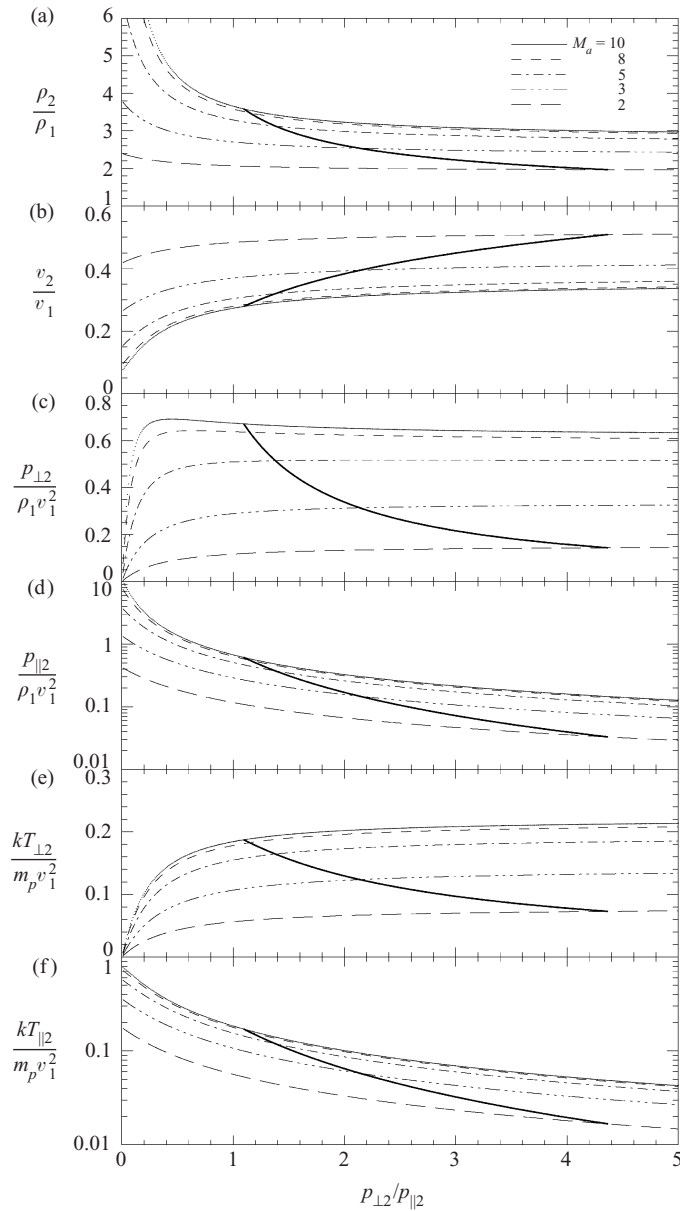


Figure 2. Plasma parameters as functions of the anisotropy rate downstream of the perpendicular shock for $A_s = 0.01$ and $\lambda_1 = 1$.

increases, and the pressure and temperature increase. One can see that the variations in density, velocity, perpendicular pressure and temperature are relatively small within the interval where the parameter λ_2 exceeds 1. However, the corresponding variations of the parallel quantities (p_{\parallel} and T_{\parallel}) are much more pronounced in this interval. In particular, taking $M_a = 2$, we estimate the variations of plasma parameters within the interval $\lambda_2 > 1$ for two values, $A_s = 0.01$ and 0.04 , as follows. The density variations are 5% and 7%, the velocity variations are 5% and 7%,

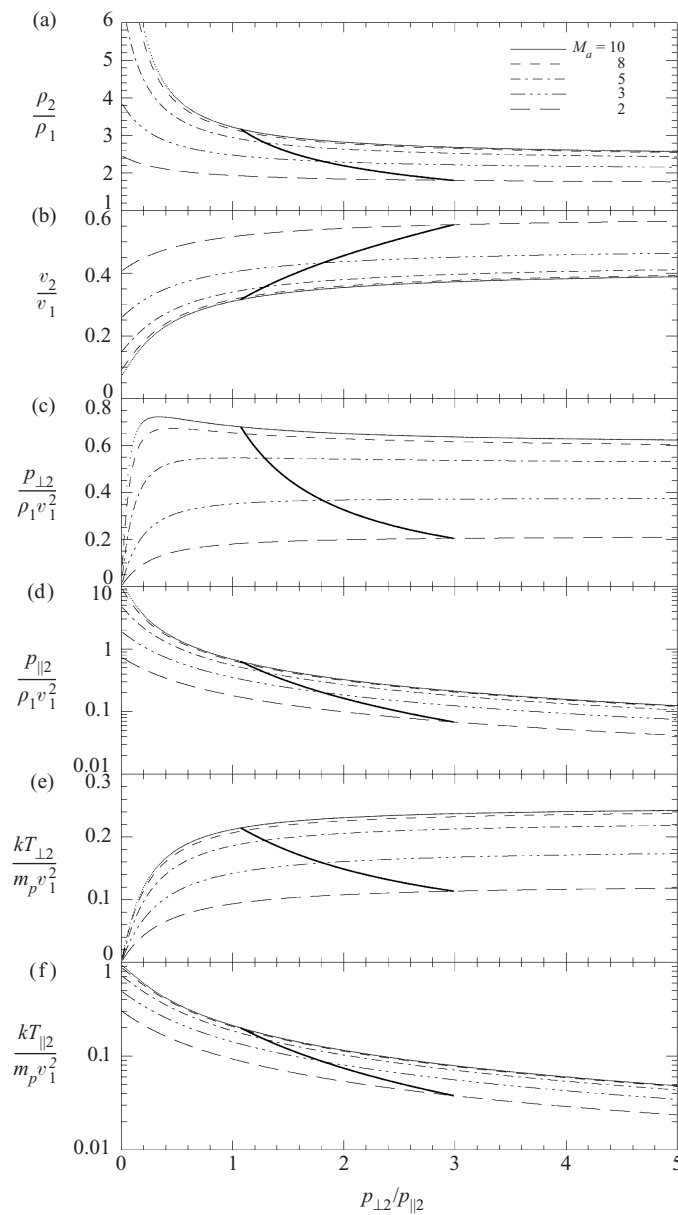


Figure 3. Plasma parameters as functions of the anisotropy rate downstream of the perpendicular shock for $A_s = 0.04$ and $\lambda_1 = 1$.

the perpendicular pressure variations are 23% and 13%, the perpendicular temperature variations are 29% and 22%, the parallel pressure variations are 72% and 62%, and the parallel temperature variations are 70% and 60%. These variations are smaller for larger values of M_a .

Figure 4 shows the density, the normal velocity, and the ratio of the perpendicular and parallel pressures obtained from the criterion for mirror instability downstream of the shock in the range of Alfvén Mach numbers $2 < M_a < 10$. Solid and dashed

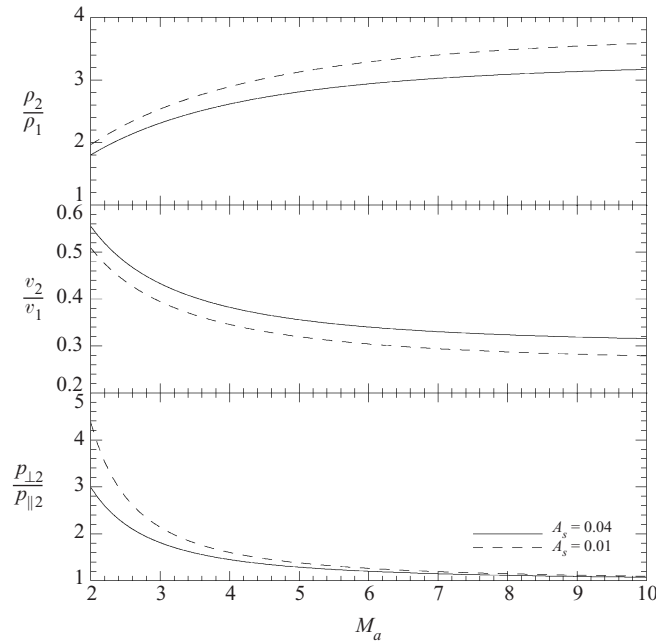


Figure 4. Density, normal component of velocity, and ratio of perpendicular and parallel pressures obtained from the criterion for mirror instability downstream of the perpendicular shock for $\lambda_1 = 1$.

lines correspond to different parameters A_s . It is an evident feature that the ratio of the pressures decreases rapidly to 1 as M_a increases. For example, this ratio is equal to 1.266, 1.150, and 1.097 for $M_a = 5$, 8, and 10 respectively. The density and normal velocity shown in Fig. 4 represent respectively minimum and maximum assessments of these quantities downstream of the anisotropic shock.

Figure 5 shows the perpendicular and parallel pressures and the perpendicular and parallel temperatures as functions of M_a , obtained downstream of the shock, taking into account the criterion for mirror instability. Solid and dashed lines correspond to different values of the parameter A_s , as in Fig. 4. For each M_a , the perpendicular temperatures shown in Fig. 5 represent maximum assessments downstream of the fast anisotropic shock. This statement is also valid for the perpendicular pressure for relatively low Alfvén Mach numbers ($M_a \leq 5$). On the other hand, the parallel pressure and temperature shown in Fig. 5 represent minimum assessments of these parameters downstream of the fast anisotropic shock. The last statement is valid for the perpendicular pressure for large M_a ($M_a > 5$).

5. Solution for inclined shocks

Next we derive the jump conditions for the general case, where the input parameters H_1 , I_1 , J_1 , and W_1 are given by (3.1)–(3.4). Thus we obtain the following expressions for B_{t2} , v_{t2} , and $p_{\perp 2}$:

$$B_{t2} = -4\pi x \frac{J_1 B_{n1} + H_1}{\varepsilon B_{n1}^2 x - 4\pi}, \quad (5.1)$$

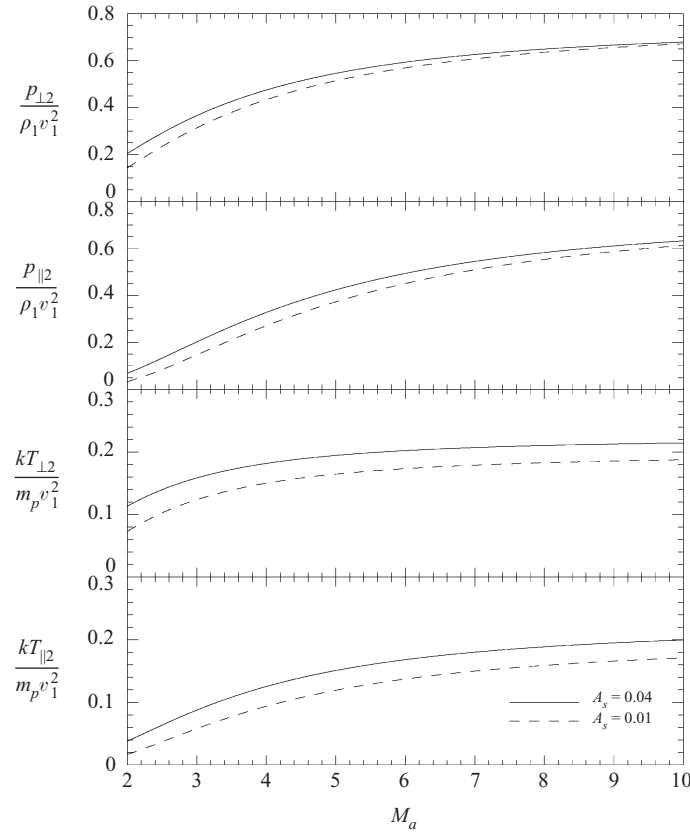


Figure 5. Perpendicular and parallel pressures and perpendicular and parallel temperatures obtained from the criterion for mirror instability downstream of the perpendicular shock for $\lambda_1 = 1$.

$$v_{t2} = -\frac{H_1}{B_{n1}} - \frac{4\pi(J_1 B_{n1} + H_1)}{B_{n1}(\varepsilon B_{n1}^2 x - 4\pi)}, \tag{5.2}$$

$$p_{\perp 2} = C[(x\varepsilon B_{n1}^2 - 4\pi)^2(4\pi x I_1 - x B_{n1}^2 + (x\varepsilon B_{n1}^2 - 4\pi)) - 8\pi^2 x^3 (J_1 B_{n1} + H_1)^2], \tag{5.3}$$

where

$$C = [4\pi x(B_{n1}^4 x^2 \varepsilon^2 - 8\pi B_{n1}^2 x \varepsilon + 16\pi^2)]^{-1}.$$

ε is defined as

$$\varepsilon = 1 - \frac{4\pi(p_{\parallel} - p_{\perp})}{B_2^2}. \tag{5.4}$$

We note that in the isotropic case ($p_{\perp} = p_{\parallel}$), it follows that $\varepsilon = 1$. Next we substitute (5.1)–(5.3) into the energy equation. Since we have introduced quantity the ε , two equations have to be solved simultaneously, namely the energy equation

$$\mathcal{A}_4 y^4 + \mathcal{A}_3 y^3 + \mathcal{A}_2 y^2 + \mathcal{A}_1 y + \mathcal{A}_0 = 0, \tag{5.5}$$

where the coefficients are given by

$$\begin{aligned}\mathcal{A}_4 &= 64\pi^3(1 + 3\lambda_2), \\ \mathcal{A}_3 &= 16\pi^3 B_{n1}^2(1 + 2\lambda_2) - 64\pi^3 I_1(1 + 4\lambda_2) - 16\pi^2 B_{n1}^2 \varepsilon(3 + 8\lambda_2), \\ \mathcal{A}_2 &= 4\pi B_{n1}^4 \varepsilon[\varepsilon(3 + 7\lambda_2) - 2(1 + 2\lambda_2)] + 32\pi^2 B_{n1}^2 I_1 \varepsilon(1 + 4\lambda_2) \\ &\quad + 64\pi^3 \lambda_2(2W_1 - J_1^2), \\ \mathcal{A}_1 &= 8\pi^2(H_1 + B_{n1}J_1)^2 + B_{n1}^6 \varepsilon^2(1 + 2\lambda_2)(1 - \varepsilon) + 32\pi^2 B_{n1}^2 \lambda_2 \varepsilon(J_1^2 - 2W_1) \\ &\quad - 4\pi B_{n1}^4 I_1 \varepsilon^2(1 + 4\lambda_2), \\ \mathcal{A}_0 &= 4\pi B_{n1}^2 \lambda_2 \varepsilon^2(2B_{n1}^2 W_1 + 2B_{n1} J_1 H_1 + H_1^2),\end{aligned}$$

and the polynomial for ε , i.e.

$$\mathcal{D}_3 \varepsilon^3 + \mathcal{D}_2 \varepsilon^2 + \mathcal{D}_1 \varepsilon + \mathcal{D}_0 = 0, \quad (5.6)$$

with the coefficients

$$\begin{aligned}\mathcal{D}_3 &= -B_{n1}^6, \\ \mathcal{D}_2 &= B_{n1}^4 [B_{n1}^2 + 4\pi y(3 - \lambda_2) - 4\pi I_1(1 - \lambda_2)], \\ \mathcal{D}_1 &= 16\pi^2 B_{n1}^2 y^2(2\lambda_2 - 3) + 8\pi B_{n1}^2 y[4\pi I_1(1 - \lambda_2) - B_{n1}^2] - 16\pi^2 \lambda_2 (J_1 B_{n1} + H_1)^2, \\ \mathcal{D}_0 &= 64\pi^3 y^2(1 - \lambda_2)(y - I_1) + 16\pi^2 B_{n1}^2 y^2 + 8\pi^2(1 + \lambda_2)(J_1 B_{n1} + H_1)^2.\end{aligned}$$

Figure 6 shows the variations of the plasma density, the normal and tangential components of the velocity, and the tangential component of the magnetic field as functions of the anisotropy parameter λ_2 downstream of the shock in the case of an inclined magnetic field for different Alfvén Mach numbers ranging from 2 to 10 and a fixed parameter $A_s = 0.01$. The angle between the normal vector and magnetic field upstream of the shock, γ , is chosen to be 45° . For the same shock, Fig. 7 shows the variations of the perpendicular and parallel pressures and temperatures versus the anisotropy rate. On the left side, all curves start from the points corresponding to the thresholds of firehose instability. Furthermore, in all panels, the thresholds of mirror instability are shown as the thick solid curves that separate stable (left from curve) and unstable (right from curve) regions in the plane of the parameters.

Figures 8 and 9 are similar to Figs 6 and 7, but correspond to a different value of the parameter A_s , namely $A_s = 0.04$. One can see from the figures that all parameters are monotonic functions of λ_2 while they exceed the value of the criterion for firehose instability. The most sensitive quantities with respect to the anisotropy parameter λ_2 are the tangential component of the velocity, the parallel pressure and the parallel temperature. Acceleration of the plasma in the direction tangential to the shock is caused by two terms: $B_n(B_{t2})/M_a^2$, and $(p_{\perp 2} - p_{\parallel 2})B_n B_{t2}/B^2$. For $\lambda_2 > 1$, the second term has the same sign as the first, and thus the tangential component of the velocity is larger than that in the case of isotropy. In the other case, where $\lambda_2 < 1$, the second term has the opposite sign, and then the tangential component of the velocity is smaller than that for isotropy. For the criterion for firehose instability, the first term is completely compensated by the second.

Figure 10 shows the density, the normal and tangential components of the velocity, and the tangential component of the magnetic field downstream of the shock as functions of the Alfvén Mach number, obtained from the criterion for mirror instability as a closure relation for the jump conditions at the shock. Solid and dashed lines correspond to different parameters A_s . It is an evident feature that it is the tangential component of the magnetic field that is most sensitive to the

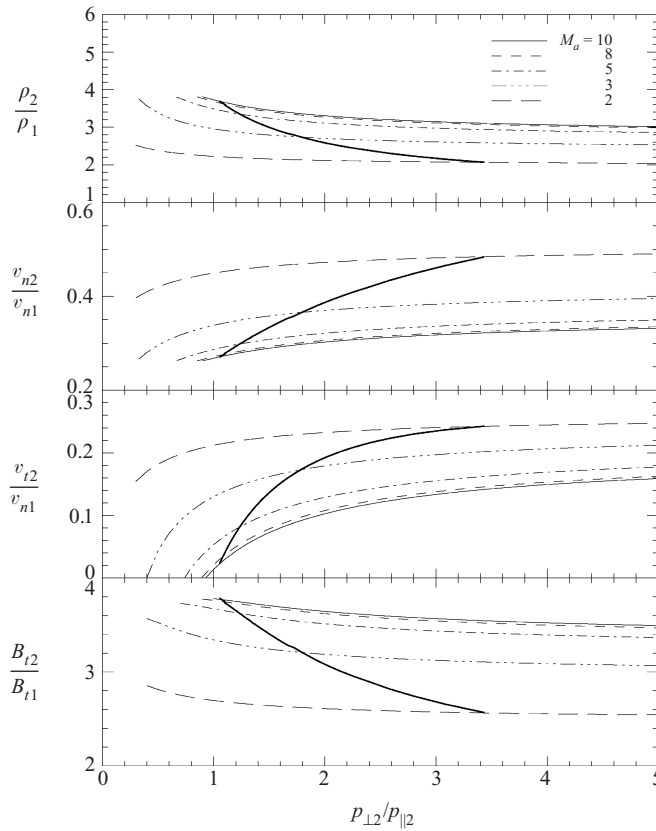


Figure 6. Density, normal and tangential components of the velocity, and tangential component of the magnetic field versus anisotropy rate downstream of the inclined shock for $A_s = 0.01$ and $\lambda_1 = 1$.

parameter A_s . For a given Alfvén Mach number, the quantities shown in Fig. 10 are minimum assessments for the density and tangential magnetic field component, and also maximum assessments for the normal and tangential components of the velocity downstream of the shock.

Finally, Fig. 11 shows the perpendicular and parallel pressures, the ratio of the pressures, and the perpendicular and parallel temperatures as functions of M_a , are obtained downstream of the shock taking account of criterion for mirror instability. Solid and dashed lines correspond to different values of the parameter A_s as in Fig. 10. For each M_a , the perpendicular temperatures and pressures shown in Fig. 11 are maximum assessments of these quantities downstream of the shock. On the other hand, the parallel pressure and temperature shown in Fig. 11 are the minimum assessments of these parameters downstream of the shock.

An interesting question is that of the variation of the entropy through the anisotropic shock. In the case of anisotropy, we have two adiabatic laws and two entropy functions corresponding to the perpendicular and parallel degrees of freedom:

$$S_{\perp} = k \ln \left(\frac{P_{\perp}}{\rho B} \right), \quad S_{\parallel} = 0.5k \ln \left(\frac{P_{\parallel} B^2}{\rho^3} \right). \quad (5.7)$$

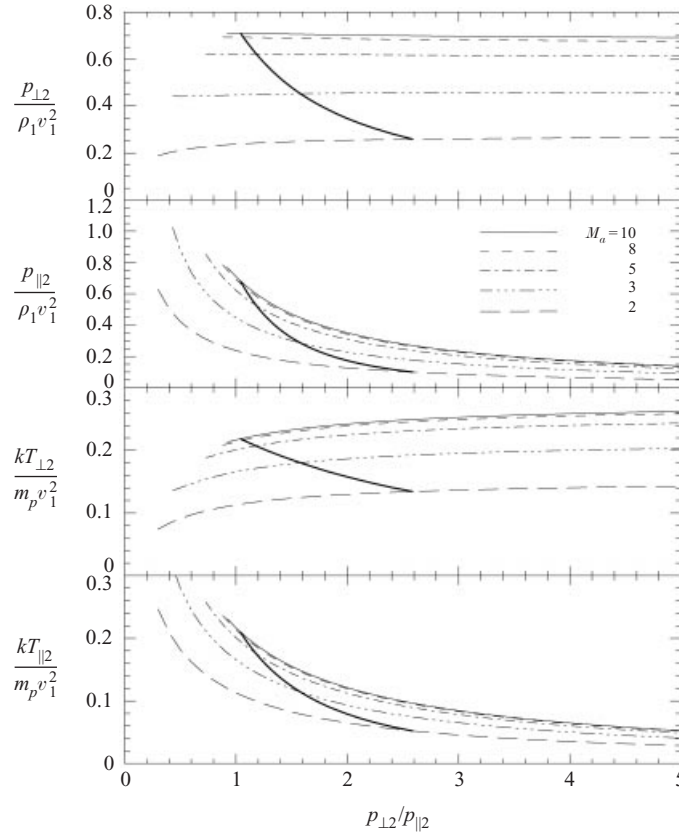


Figure 7. Perpendicular and parallel pressures and perpendicular and parallel temperatures versus anisotropy rate downstream of the inclined shock for $A_s = 0.01$ and $\lambda_1 = 1$.

Here the entropies are referred to one particle, and k is the Boltzmann’s constant.

Inside the shock front, the kinetic energy is converted into thermal energy and the variations of the entropy functions are caused by heat fluxes,

$$T_{\parallel} dS_{\parallel} = q + q_1, \quad T_{\perp} dS_{\perp} = -q + q_2. \tag{5.8}$$

Here q_1 and q_2 are the positive external heat fluxes, and q is the exchange heat flux between perpendicular and parallel degrees of freedom.

From the equations (5.8) we find

$$dS_{\parallel} = \frac{q + q_1}{T_{\parallel}}, \quad dS_{\perp} = \frac{-q + q_2}{T_{\perp}}. \tag{5.9}$$

Adding together the two equations in (5.9), we obtain the differential of the total entropy:

$$dS = \frac{q(T_{\perp} - T_{\parallel})}{T_{\perp}T_{\parallel}} + \frac{q_1}{T_{\parallel}} + \frac{q_2}{T_{\perp}} > 0, \tag{5.10}$$

where

$$S = S_{\parallel} + S_{\perp} = 0.5k \ln \left(\frac{P_{\perp}^2 P_{\parallel}}{\rho^5} \right). \tag{5.11}$$

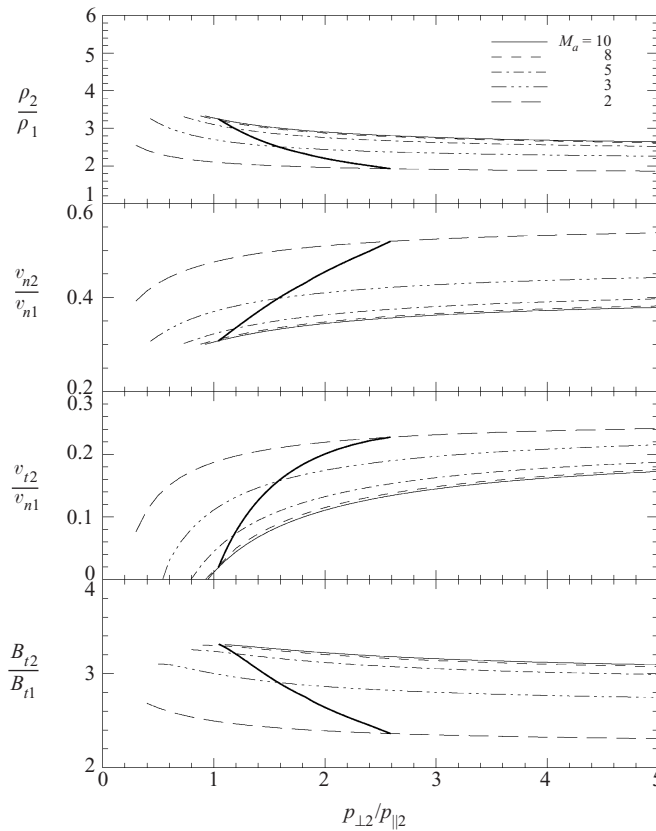


Figure 8. Density, normal and tangential components of the velocity, and tangential component of the magnetic field versus anisotropy rate downstream of the inclined shock for $A_s = 0.04$ and $\lambda_1 = 1$.

On the right-hand side of (5.10), the second term is obviously positive because it is proportional to the heat flux related with dissipation of kinetic energy of the plasma flow. The first term is proportional to the heat flux from the perpendicular to the parallel energy. It follows from thermodynamics that this heat flux must be positive when $T_{\perp} > T_{\parallel}$ and negative when $T_{\perp} < T_{\parallel}$. Therefore, in all cases, the first term in (5.10) must be positive, and hence the variation of the total entropy through the shock front must be positive.

This thermodynamic condition is checked in our solution. Figure 12 shows the total entropy difference at the fast shock as a function of the anisotropy rate for a range of Alfvén Mach numbers and to our values of the parameters A_s . All plots indicate the positive difference of the total entropy defined by (5.11) in the whole range of the anisotropy rate, with a shallow maximum at the point corresponding to the case of isotropy. This behaviour is in agreement with the thermodynamic law.

6. Discussion and conclusions

We have solved the system of jump conditions for the fast shock in a magnetized anisotropic plasma, taking into account the criteria for mirror and firehose instabil-

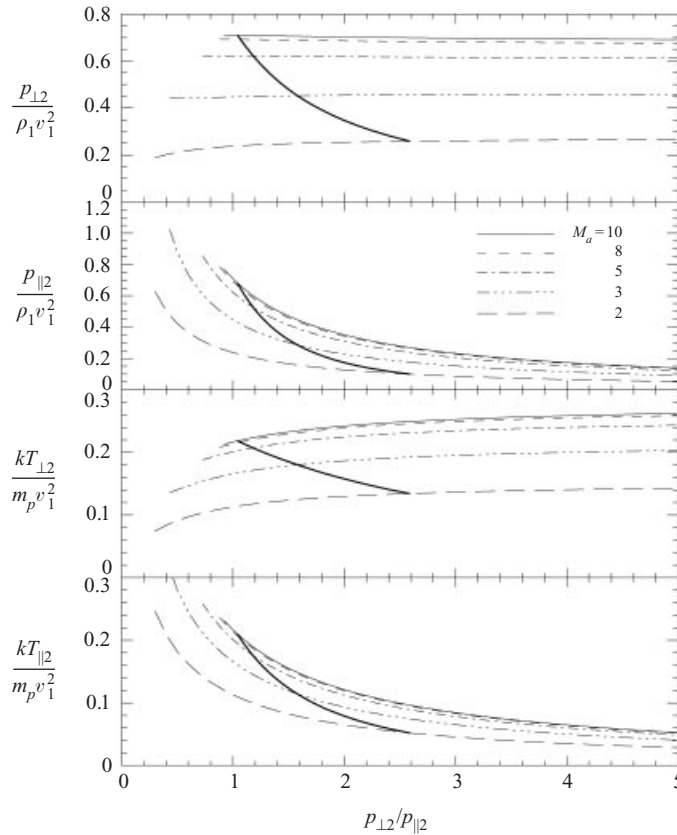


Figure 9. Perpendicular and parallel pressures and perpendicular and parallel temperatures versus anisotropy rate downstream of the inclined shock for $A_s = 0.04$ and $\lambda_1 = 1$.

ities bounding the pressure anisotropy downstream of the shock. Taking different upstream dimensionless parameters M_a in a range from 2 to 10 and $A_s = 0.01$ and 0.04, all plasma parameters and magnetic field downstream of the shock are obtained as functions of the anisotropy rate defined as the ratio of perpendicular and parallel pressures.

For the perpendicular shock, the mirror instability bounds the maximum anisotropy rate. But, in this case, the firehose instability plays no role as a bounding factor for low anisotropy rate. When the anisotropy parameter λ_2 goes to zero, the density, parallel pressure, and parallel temperature increase strongly, especially for high Alfvén Mach numbers. This feature can be easily explained from the conservation equations for normal momentum flux, mass flux, and tangential electric field. In the limiting case $p_{\perp} \rightarrow 0$ and $A_s = 0$, the dimensionless conservation equation is given by

$$\frac{\rho_2 v_2^2}{\rho_1 v_1^2} + \frac{B_2^2}{2M_a^2} = 1 + A_s + \frac{1}{2M_a^2}. \tag{6.1}$$

Using the equation of mass conservation, $\rho_1 v_1 = \rho_2 v_2$, we obtain a quadratic equation and finally a simple expression for the density jump:

$$\frac{\rho_2}{\rho_1} = \frac{1}{2}(\sqrt{1 + 8M_a^2} - 1).$$

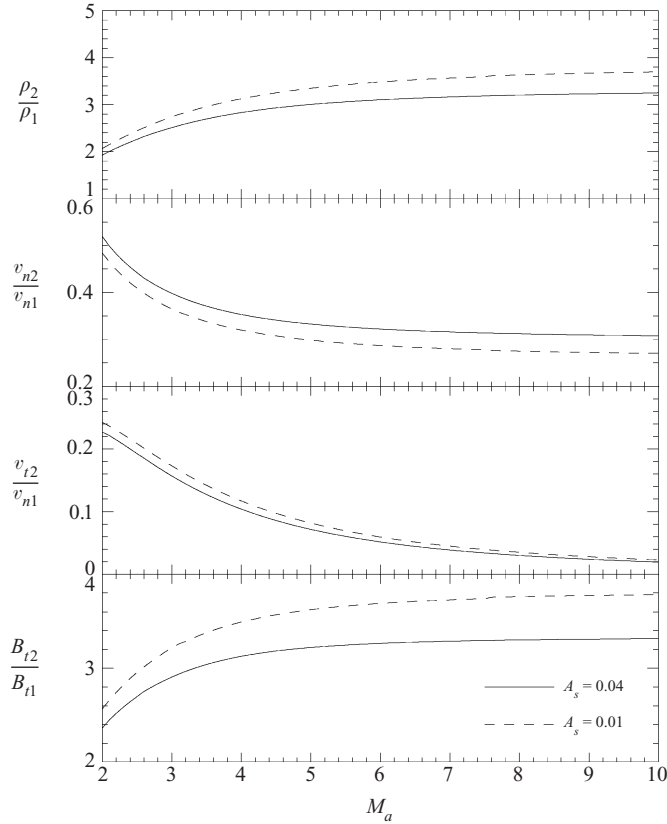


Figure 10. Density, normal and tangential components of velocity, and tangential component of magnetic field obtained from the criterion for mirror instability downstream of the inclined shock for $\lambda_1 = 1$.

This simple analytical formula agrees with the large enhancement of the density shown in Fig. 2 for low anisotropy rate and high Alfvén Mach numbers.

For the perpendicular shock, another limiting case, namely, $p_{\perp}/p_{\parallel} \rightarrow \infty$ and $A_s = 0$, can also be described analytically. This limiting case corresponds to the solution of the usual MHD Rankine–Hugoniot jump conditions (Weitzner 1983) for polytropic index $\kappa = 2$. In this case, the density is given by the formula

$$\frac{\rho_2}{\rho_1} = \frac{3}{1 + 2/M_a^2}.$$

This formula is applicable only for a very small parameter A_s when the anisotropy of the plasma pressure upstream of the shock has negligible influence on the parameters downstream of the shock.

We have examined the solution for an inclined shock that has an angle of 45° between the magnetic field and the normal vector of the discontinuity. In the case of the inclined shock, the minimum anisotropy rate is bounded by the criterion for firehose instability. Thus the limit $p_{\perp} \rightarrow 0$ has no physical sense for the inclined shock. Some parameters have relatively small variations as functions of the anisotropy parameter λ_2 . These are the density, the normal component of the velocity, the tangential component of the magnetic field, the perpendicular pressure, and

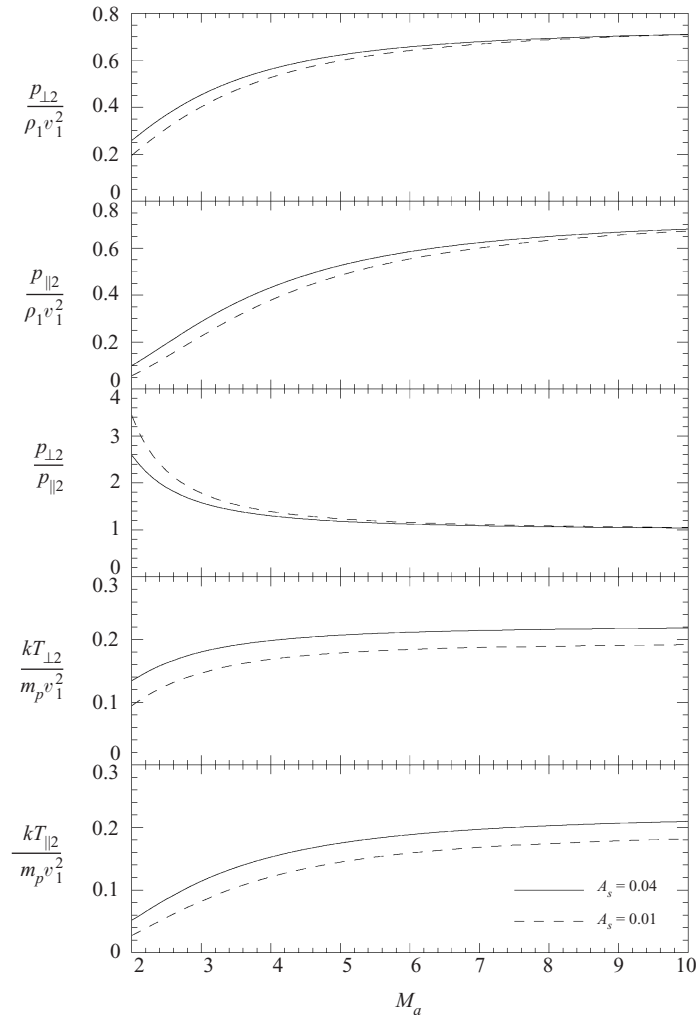


Figure 11. Perpendicular and parallel pressure, anisotropy rate, and perpendicular and parallel temperature obtained from the criterion for mirror instability downstream of the inclined shock for $\lambda_1 = 1$.

the perpendicular temperature. Variations of other parameters, such as the parallel pressure, the parallel temperature, and the tangential component of the velocity, are much more pronounced as functions of the anisotropy rate downstream of the shock. The anisotropy rate upstream of the shock has a minor effect in the case of a small parameter A_s , as considered in this paper.

The total entropy is defined for an anisotropic plasma as the sum of entropies corresponding to the parallel and perpendicular degrees of freedom. This total entropy is shown to increase through the fast shock front for the whole range of anisotropy rates and Alfvén Mach numbers used in our study. For given Alfvén and sonic Mach numbers, the entropy growth at the shock has a maximum for an anisotropy rate equal to 1. The latter corresponds to the case of isotropy when the perpendicular and parallel temperatures are completely relaxed.

Observations of field and plasma behaviour in the solar wind as well as in the

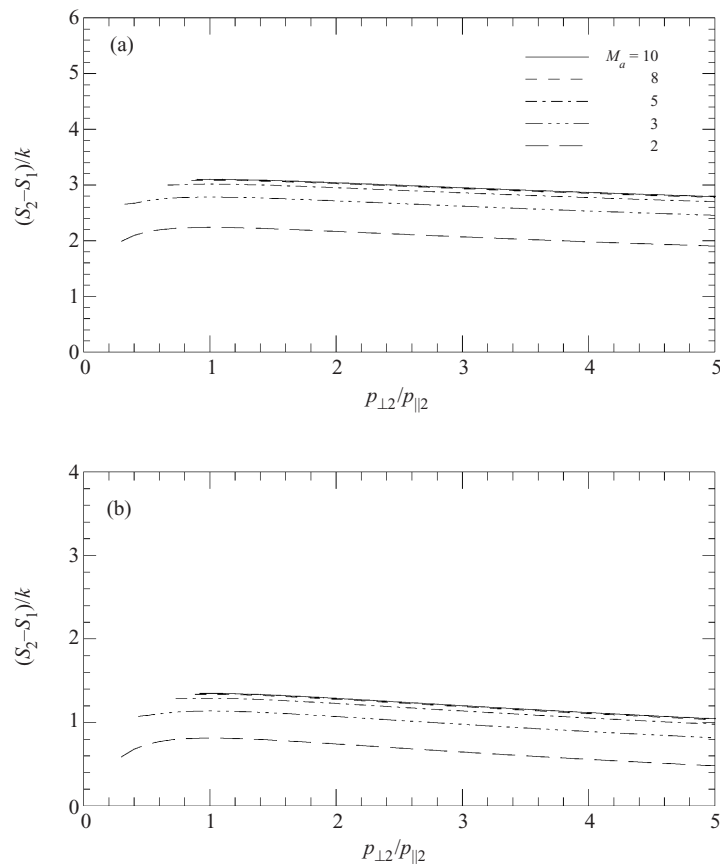


Figure 12. Total entropy difference as function of the anisotropy rate downstream of the shock for $\lambda_1 = 1$, for different Alfvén Mach numbers and (a) $A_s = 0.01$ and (b) $A_s = 0.04$.

Earth's magnetosheath have highlighted the need to develop a MHD flow model where the plasma pressure is treated as a tensor. It is seen in many spacecraft measurements (see e.g. Anderson and Fuselier 1993; Phan et al. 1994) that the ratio of perpendicular and parallel plasma pressures is usually larger than 1. The range of parameters A_s and M_a chosen in our study is quite typical for solar wind conditions. In this respect, the results of our paper are expected to be useful for the interpretation of fast shocks propagating in space plasmas. The Earth's bow shock has anisotropy features directly measured by spacecraft. The ratio of perpendicular and parallel temperatures downstream of the shock varies from event to event, but is usually larger than 1. The anisotropy rate usually does not exceed the limit corresponding to the mirror threshold. Mirror modes produced by the temperature anisotropy are typically indicated by observations in the flow region downstream of the shock. Thus the closure relation based on the mirror instability criterion agrees with observations in most of the magnetosheath (the region between the bow shock and the magnetospheric boundary), where the plasma beta is larger than 1.

Acknowledgements

Part of this work was done while N. V. E. was on a research visit to the Space Research Institute of the Austrian Academy of Sciences in Graz, and H. K. B. and

D. F. V. were on a research visit to the Institute of Computational Modelling of the Russian Academy of Sciences in Krasnoyarsk, Siberia. D. F. V. acknowledges support for this visit from the mayor of Wolfsberg, Austria. This work is supported by INTAS-ESA Project 99-01277, by Grant 98-05-65290 from the Russian Foundation of Basic Research, by Grant 97-0-13.0-71 from the Russian Ministry of Education, by the Austrian Fonds zur Förderung der wissenschaftlichen Forschung under Project P12761-TPH, and by the Austrian Academy of Sciences, 'Verwaltungsstelle für Auslandsbeziehungen'.

References

- Abraham-Shrauner, B. 1967 Shock jump conditions for an anisotropic plasma. *J. Plasma Phys.* **1**, 379.
- Anderson, B. J. and Fuselier, S. A. 1993 Magnetic pulsations from 0.1 to 4.0 Hz and associated plasma properties in the Earth's subsolar magnetosheath and plasma depletion layer. *J. Geophys. Res.* **98**, 1461.
- Chew, G. F., Goldberger, M. L. and Low, F. E. 1956 The Boltzmann equation and the one-fluid hydromagnetic equations in the absence of particle collisions. *Proc. R. Soc. Lond.* **A236**, 112.
- Hudson, P. D. 1970 Discontinuities in an anisotropic plasma and their identification in the solar wind. *Planet. Space Sci.* **18**, 1611.
- Lynn, Y. M. 1967 Discontinuities in an anisotropic plasma. *Phys. Fluids* **10**, 2278.
- Neubauer, F. M. 1970 Jump relations for shocks in an anisotropic magnetized plasma. *Z. Phys.* **237**, 205.
- Phan, T.-D., Paschmann, G., Baumjohann, W. and Sckopke, N. 1994 The magnetosheath region adjacent to the dayside magnetopause: AMPTE/IRM observations. *J. Geophys. Res.* **99**, 121.
- Thompson, W. B. 1964 *An Introduction to Plasma Physics*, p. 216. Pergamon, New York.
- Tajiri, M. 1967 Propagation of hydromagnetic waves in collisionless plasma, II, Kinetic approach. *J. Phys. Soc. Jpn.* **22**, 1482.
- Weitzner, H. 1983 Linear wave propagation in ideal magnetohydrodynamics. In: *Handbook of Plasma Physics*, Vol. 1 (ed. A. A. Galeev and R. N. Sudan), p. 201. North-Holland, Amsterdam.